Pressure induced complexity in a lithium monolayer: *Ab initio* calculations

A. Rodriguez-Prieto and A. Bergara

Materia Kondentsatuaren Fisika Saila, Zientzia eta Teknologia Fakultatea, Euskal Herriko Unibertsitatea, 644 Postakutxatila, 48080 Bilbo, Basque Country, Spain and Donostia International Physics Center (DIPC), Paseo de Manuel Lardizabal, 20018, Donostia, Basque Country, Spain

(Received 26 January 2005; revised manuscript received 11 May 2005; published 2 September 2005)

Light alkali metals have usually been considered as *simple* metals due to their monovalency and high conductivity. In these metals ionic pseudopotentials are weak and the nearly free electron model (NFE) becomes quite accurate at normal conditions. However, very recent experiments have shown that at high pressures their electronic properties deviate radically from the NFE model and even become unexpected good superconductors. In this work we present *ab initio* calculations to analyze the deviation from simplicity in a lithium monolayer (ML) when pressure is applied. We have seen that as a result of the increasing nonlocal character of the atomic pseudopotential with increasing pressure, the surprising half filling tight bindinglike nesting observed in the Fermi *line* can explain the interesting *complex* behavior in a lithium ML, induced by its correlated structural, electronic, and even magnetic properties.

DOI: 10.1103/PhysRevB.72.125406 PACS number(s): 71.18.+y, 71.15.Mb, 68.35.−p, 73.20.At

I. INTRODUCTION

Light alkalies are usually considered as *simple* metals, because as a consequence of the weak interaction between valence electrons and ionic cores, under normal conditions they crystallize in simple high symmetric structures. Therefore, the nearly free electron model (NFE) has been considered a good approximation to describe their electronic properties.[1] The only exception is hydrogen which, even when it solidifies, forms very stable diatomic molecules and presents an insulating character. However, recent results, both theoretical and experimental, have changed our perception of the alkalies and have shown that the NFE model breaks when high pressures are applied. Neaton *et al.* reported *ab initio* calculations for bulk lithium[2] and predicted that pressure could induce structural transitions to less symmetric, lower coordinated structures, associated with electronic localizations. These theoretical predictions have been confirmed by experiments,[3] finding that around 40 GPa a phase transition to a complex structure ($cI16$) with 16 atoms per unit cell occurs. It is important to notice that pressure induced transitions from simple to more complex structures are not singular to lithium but have also been predicted in heavier alkalies.[4,5] On the other hand, other very recent experiments[6–8] have also shown that at this pressure range lithium presents a superconducting transition with $T_c \sim 20$ K, becoming the highest transition temperature between simple elements.[9] It is noteworthy that experiments looking for superconductivity in lithium under ambient pressure have failed.[10] This even raises the interest to characterize the physical properties of compressed lithium close to the observed electronic and structural transitions.

In this article we present an *ab initio* theoretical analysis of the pressure-induced structural, electronic, and even magnetic properties of a single lithium ML, with the atoms confined to move in the plane. The development of new techniques for the atomic manipulation[11,12] allows the growth of atomic monolayers on inert substratum, semiconductors, or noble gases, which rises the interest to analyze physical properties of low dimensional systems under different conditions. In addition, it may be possible to study single MLs of variable density by depositing the atoms through implementation of a *sandwich* geometry between inert substrates. On the other hand, the simplicity of the atomic configuration associated with the ML facilitates the performing of a more detailed analysis, and extending our conclusions to the bulk will also provide an interesting perspective to understand the physical origin of the experimentally observed features of compressed lithium. In Sec. II we describe the theoretical and computational background of this work. Results and conclusions will be presented in Secs. III and IV, respectively.

II. THEORETICAL AND COMPUTATIONAL BACKGROUND

In order to describe structural and electronic properties of a lithium ML over a wide range of densities we have used a plane-wave implementation of the density-functional theory (DFT) (Refs. 13 and 14) within the local density approximation (LDA) (Refs. 15–17) for nonmagnetic calculations and local spin density approximation (LSDA) (Ref. 18) to analyze the magnetic properties of the ML. All calculations have been performed with the Vienna *Ab initio* Simulation Package (VASP).[19,20] Effects of compression were simulated by reducing the lattice parameter. As the atomic spacing is reduced a significant core overlap is observed, so that we have required methods which take into account core electrons. For fully treating them we make use of the projector augmented wave (PAW) method.[21] A Monkhorst–Pack[22] mesh of $20\times20\times1$ has been chosen for the sampling of the Brillouin zone. The description of the ML is implemented by a supercell which, in order to minimize interactions between MLs, contains ten layers of vacuum between MLs. The ions are relaxed to their equilibrium positions by calculating the forces acting on them using the Hellmann-Feynmann theorem. In all the calculations we have used an energy cutoff of $E_{\text{cut}} \simeq 815$ eV.

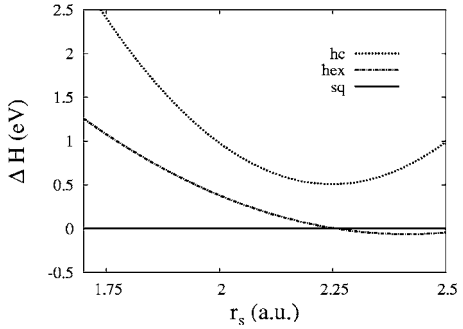

FIG. 1. Enthalpy $H=E+\sigma A$, σ being the surface tension: $\sigma=-dE/dA$, as a function of the density parameter r_s for three simple structures: hexagonal (hex), square (sq) and honeycomb (hc). All enthalpies are referenced to the square structure, $\Delta H=H-H_{\mathrm{sq}}$.

III. RESULTS

A. Structural and electronic analysis

Following the analysis in Ref. 23, as a first step we will just consider three simple structures of a lithium ML: hexagonal (hex), square (sq), and honeycomb (hc). In the case of the hex and sq structures we consider monatomic unit cells and the hc structure is implemented by using a graphitelike unit cell with a two-atom basis. Figure 1 shows the calculated enthalpies for these structures. As it is a common property of the alkalies, lithium ML at equilibrium, $r_s=3.02$ a.u. [r_s is the two-dimensional linear density parameter, defined by the relation $A/N=\pi(r_s a_0)^2$, where N is the number of nuclei in a ML with area A and a_0 is the Bohr radius], also favors the compact hexagonal structure (hex). However, as we can observe in Fig. 1, at $r_s<2.25$ a.u. the more open square structure (sq) becomes favored over the hexagonal one.

In Fig. 2 we plot the band structure and density of states (DOS) of a lithium ML corresponding to the hexagonal structure at equilibrium and the square structure with $r_s=2.15$ a.u., just after the structural transition. At equilibrium [Fig. 2(a)] only one band is occupied, which is characterized by a parabolic-type dispersion of s character, as corresponds to a good NFE-like system. For occupied energies the DOS is almost constant, which reflects the quasi-two-dimensional character of the ML. However, at higher pressures [Fig. 2(b)] the first band flattens associated with the increasing of the band gap at the zone boundary, indicating a clear electronic localization. The energy difference between the first two bands at Γ decreases so much that the p_z band, antisymmetric in the direction perpendicular to the ML, starts to be occupied and opens a new conduction channel. It is also interesting to note that the van Hove singularities lie close to the Fermi energy which, therefore, raises the DOS. All these interesting characteristics can only be explained in terms of the nonlocal character of the ionic pseudopotential.[23]

Another essential feature determining electronic properties of the ML is the geometry associated with the Fermi line, which is displayed in Fig. 3 for the same densities and structures as above. At equilibrium just one Fermi line exists, associated with the s band, which is almost circular as corresponds to a NFE approximation. However, as mentioned

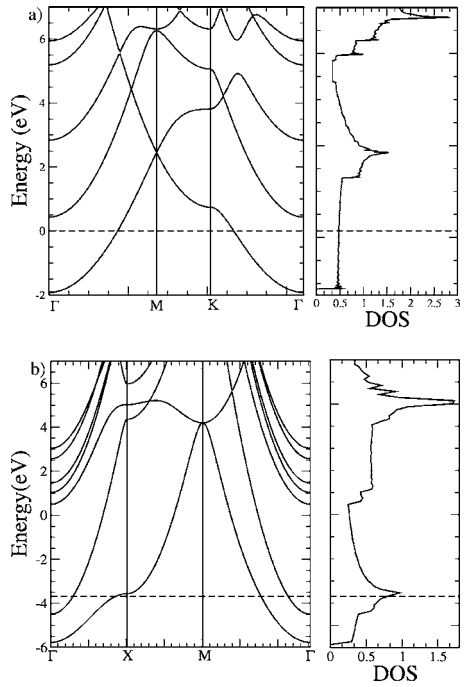

FIG. 2. Band structure and density of states (DOS) for (a) a hexagonal lithium ML at equilibrium ($r_s=3.02$ a.u.) and (b) a square structure with $r_s=2.15$ a.u. The Fermi energy is represented by the dotted line.

above, this simple picture breaks at higher densities. At $r_s=2.15$ a.u. there are two Fermi lines associated with the two occupied s and p_z bands and, surprisingly, the Fermi line associated with the s band becomes a perfect square as corresponds to a half filled tight bindinglike model. As it is well known, this model becomes appropriate to describe electronic properties of systems with localized electronic states, just being the opposite case to the NFE approximation valid at normal pressures. The perfect nesting observed at $r_s=2.15$ a.u. strongly couples electronic states close to the Fermi line along the $\overline{\Gamma M}$ direction, and might induce structural Peierls transitions.

B. Peierls transition

As a consequence of the nesting in the Fermi line at $r_s\simeq 2.15$ a.u., any perturbation which breaks the electronic degeneration might be favored. Although different symmetry breaking perturbations might be proposed, in this section we have included the analysis of the two simplest diatomic square structures: dsq_1 and dsq_2. In both structures we start from a diatomic square unit cell, with atoms located at the vertex and the center of the square, and allow the central atom to move along two highly symmetric directions in the ML: the nearest neighbor (dsq_1) and second nearest neighbor (dsq_2) directions.

In Fig. 4 we present the enthalpies as a function of the density for the five structures considered: hc, hex, sq, dsq_1 and dsq_2. It is interesting to note that at $r_s\simeq 2.15$ a.u., just the density where the nesting in the Fermi line of the monatomic square structure (sq) is found, the new dsq_2 structure pro-

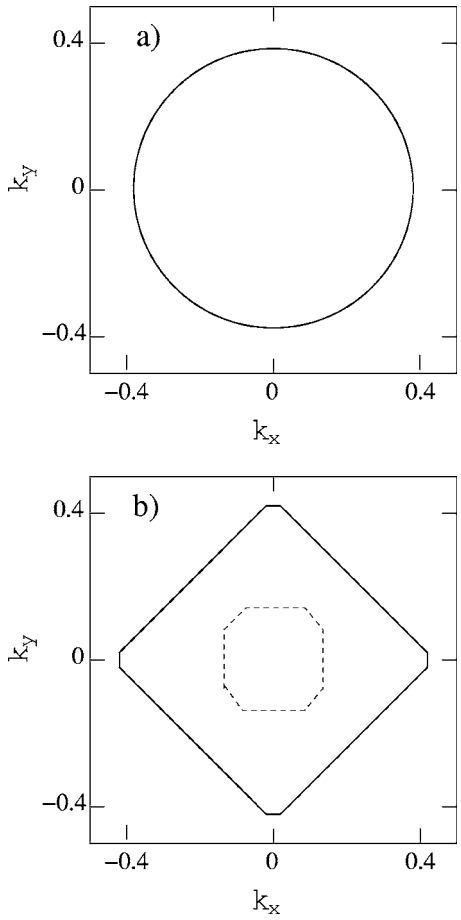

FIG. 3. Fermi lines of (a) a hexagonal lithium ML at equilibrium and (b) a square ML with $r_s=2.15$ a.u. The solid line corresponds to the Fermi line of the s band and the dotted line is associated with the p_z band, which becomes occupied at high densities.

posed in this work is favored over the others. Therefore, the perturbation caused by the nesting in the Fermi line consists of a relative movement of the atoms in the second nearest neighbor direction, producing a charge density wave in this direction. However, at much higher densities ($r_s=1.35$ a.u.)

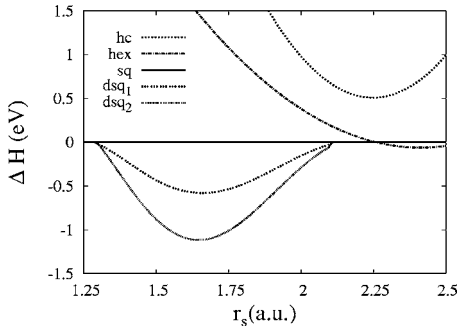

FIG. 4. Entalphy as a function of the density parameter, r_s, for all the structures considered: hc, hex, sq, dsq_1 and dsq_2. All the enthalpies are referenced to the square enthalpy, $\Delta H=H-H_{sq}$. Although the sq structure becomes favored at $r_s=2.25$ a.u., the proposed new diatomic square structure (dsq_2), where the atom at the center is allowed to move along the direction of the second nearest neighbor, is preferred at higher densities (1.3 a.u. $<r_s<2.15$ a.u.).

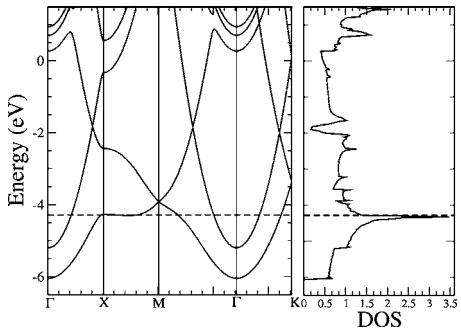

FIG. 5. Band structure and DOS of a lithium ML with dsq_2 structure at $r_s=2.0$ a.u. The s band becomes extraordinarily flat in the $\overline{XM}$ direction.

the sq structure is favored again over the diatomic structures.

Figure 5 shows the band structure and DOS for the dsq_2 structure at $r_s=2.0$ a.u., which confirms the clear deviation from a NFE behavior, already manifested for the monatomic structures of a lithium ML. The s band amazingly flattens in the $\overline{XM}$ direction, which indicates a strong electronic localization in this direction, although the ML remains metallic. In Fig. 6 we plot the LDA valence charge density of the dsq_2 structure at $r_s=2.0$ a.u. The charge density accumulates between the ions forming a clear one-dimensional conducting channel, which also originates in a very sharp singularity in the electronic DOS close to the Fermi energy (Fig. 5).

In order to characterize the phase transition involving the dsq_2 structure we have analyzed the displacement of the central atom along the minimum energy direction as a function of the density. As it is shown in Fig. 7 and expected from our analysis above, the atomic displacement is zero for $r_s>2.15$ a.u. However, at $r_s=2.15$ a.u. the high anharmonic potential of the central atom induces the presence of a soft phonon mode which moves the atom at the center. As it is displayed in Fig. 7, around $r_s=2.15$ a.u. the displacement of the central atom grows continuously with increasing density,

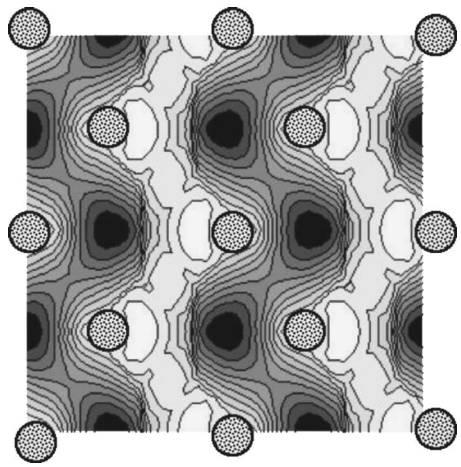

FIG. 6. LDA valence charge density of the proposed dsq_2 lithium ML at $r_s=2.0$ a.u. The ions with core electrons are represented by circles with dots inside, while the valence charge density maximum (black areas) accumulates between them, forming a clear one-dimensional conducting channel.

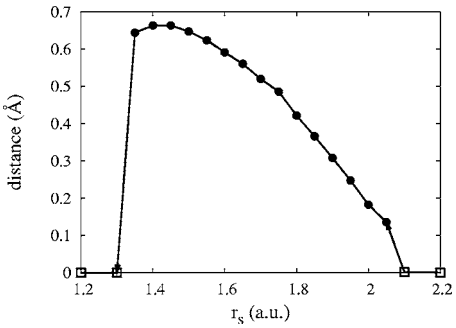

FIG. 7. Displacement of the central atom in the dsq_2 structure (solid dots) along the second nearest neighbor direction as a function of the density. The open squares correspond to the sq structure, where the atom remains at the center.

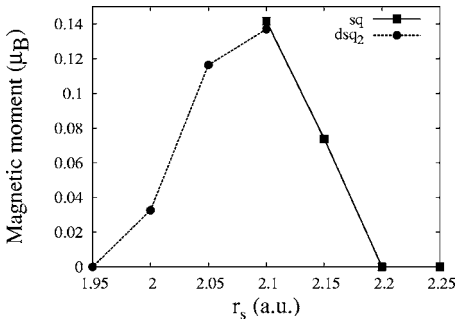

FIG. 8. Magnetic moment per atom as a function of the density, r_s, for a lithium ML with sq (squares) and dsq_2 (dots) structures, which minimize the energy at the pressure range considered. Lithium ML presents a stable ferromagnetic ground state in the proximities of the Peierls transition, with a maximum net magnetic moment per atom of $\sim 0.14\ \mu_B$, located close to the density where the structural transition ($sq \rightarrow dsq_2$) has been predicted, $r_s = 2.1$ a.u.

which indicates the second-order character of the $sq \rightarrow dsq_2$ transition. However, if we keep rising the density, we find that at $r_s \simeq 1.3$ a.u. the displacement of the central atom vanishes discontinuously and the ML goes back to the monatomic sq structure. We have seen that this transition is explained by the presence of an absolute minimum energy at the center while relative minima at finite displacements from the center still remain, characterizing the $dsq_2 \rightarrow sq$ transition as first order.

C. Magnetic instability

In a low density electron gas it is well known that a ferromagnetic instability can be induced as the kinetic energy penalty in the ferromagnetic state is compensated by the gain associated with the electronic exchange.[24] Thus, in principle, we would not expect such a transition to occur for high densities. However, as we can see in Figs. 2 and 5, the second band starts to be occupied as density is increased. Therefore, the effective low electronic density in the p_z band, in conjunction with the high DOS in the proximities of the Fermi energy and the nesting observed in the Fermi line, could induce a ferromagnetic instability in a lithium ML. Figure 8 displays *ab initio* calculations within the LSDA approximation which predict that a ferromagnetic instability can occur in a narrow density range: 2.2 a.u. $> r_s >$ 1.95 a.u. It is interesting to notice that the maximum value of the net magnetic moment per conduction electron, $\sim 0.14 \mu_B$, is observed at $r_s = 2.1$ a.u., just at the density where the $sq \rightarrow dsq_2$ Peierls structural transition takes place. This magnetic instability in a lithium ML, which has been shown to be correlated with electronic and structural transitions presented above, also proves the complexity that pressure induces in these, otherwise considered, simple systems.

IV. CONCLUSIONS

In summary, according to the *ab initio* calculations presented in this work, although the NFE model correctly describes the properties of the lithium ML at normal conditions, it loses its validity as the electronic density increases. We have analyzed pressure-induced complexity in structural, electronic and even magnetic properties of the ML, finding an interesting correlation between them. As density goes up, a flattening of the *s* band is observed, indicating an electronic localization. The corresponding nesting in the Fermi line and van Hove singularities in the proximities of the Fermi energy observed at $r_s \simeq 2.1$ a.u. induce a Peierls second-order structural transition ($sq \rightarrow dsq_2$). Beyond these features, at around the same density, the nonlocal character of the ionic pseudopotential allows us to start filling the p_z band, and its low effective initial occupation causes a ferromagnetic Bloch instability. Besides the intrinsic interest of studying the physical properties of systems with reduced dimensionality, the simplicity of the ML allows us to make a more detailed analysis and by extending these conclusions to bulk systems will provide us a very useful perspective to understand the physical origin of the complexity observed in compressed bulk lithium.[25]

ACKNOWLEDGMENT

A. Rodriguez-Prieto would like to acknowledge financial support from the Basque Hezkuntza, Unibertsitate eta Ikerketa Saila.

[1] E. Wigner and F. Seitz, Phys. Rev. **43**, 804 (1933).
[2] J. B. Neaton and N. W. Ashcroft, Nature (London) **400**, 141 (1999).
[3] M. Hanfland, K. Syassen, N. E. Christensen, and D. L. Novikov, Nature (London) **408**, 174 (2000).
[4] J. B. Neaton and N. W. Ashcroft, Phys. Rev. Lett. **86**, 2830 (2001).
[5] N. E. Christensen and D. L. Novikov, Solid State Commun. **119**,

477 (2001).
[6] K. Shimizu, H. Ishikawa, D. Takao, T. Yagi, and K. Amaya, Nature (London) **419**, 597 (2002).
[7] V. V. Struzhkin, M. I. Eremets, W. Gan, H. K. Mao, and R. J. Hemley, Science **298**, 1213 (2002).
[8] S. Deemyad and J. S. Schilling, Phys. Rev. Lett. **91**, 167001 (2003).
[9] N. W. Ashcroft, Nature (London) **419**, 569 (2002).
[10] K. I. Juntunen and J. T. Tuoriniemi, Phys. Rev. Lett. **93**, 157201 (2004).
[11] H. Uchida, D. Huang, F. Grey, and M. Aono, Phys. Rev. Lett. **70**, 2040 (1993).
[12] C. T. Salling and M. G. Lagally, Science **265**, 502 (1994).
[13] P. Hohenberg and W. Kohn, Phys. Rev. **136**, B864 (1964).
[14] W. Kohn and L. J. Sham, Phys. Rev. **140**, A1133 (1965).
[15] D. M. Ceperley and B. J. Alder, Phys. Rev. Lett. **45**, 566 (1980).
[16] J. P. Perdew and A. Zunger, Phys. Rev. B **23**, 5048 (1981).
[17] J. P. Perdew and Y. Wang, Phys. Rev. B **45**, 13244 (1992).
[18] O. Gunnarson and B. I. Lundqvist, Phys. Rev. B **13**, 4274 (1976).
[19] G. Kresse and J. Hafner, Phys. Rev. B **47**, R558 (1993).
[20] G. Kresse and J. Furthmüller, Phys. Rev. B **54**, 11169 (1996).
[21] P. E. Blöchl, Phys. Rev. B **50**, 17953 (1994).
[22] H. J. Monkhorst and J. D. Pack, Phys. Rev. B **13**, 5188 (1976).
[23] A. Bergara, J. B. Neaton, and N. W. Ashcroft, Phys. Rev. B **62**, 8494 (2000).
[24] F. Bloch, Z. Phys. **57**, 545 (1929).
[25] A. Rodriguez-Prieto and A. Bergara (to be published).